Flowing Afterglow Studies of the Temperature Dependencies for Dissociative Recombination of O_2^+, CH_5^+, $C_2H_5^+$, and $C_6H_7^+$ with Electrons

Jason L. McLain, Viktoriya Poterya, Christopher D. Molek, Lucia M. Babcock, and Nigel G. Adams*

Department of Chemistry, University of Georgia, Athens, Georgia 30602

Received: March 15, 2004; In Final Form: May 14, 2004

A temperature-variable flowing afterglow with an electrostatic Langmuir probe has been used to determine the rate coefficients, α_e, for the recombination of a series of molecular ions with electrons. The α_e for O_2^+, CH_5^+, $C_2H_5^+$, and $C_6H_7^+$ have been determined at temperatures ranging from 80 to 600 K. Data for O_2^+ over the temperature range of 100−500 K establish a single-power law dependence, which is consistent with previous data in this temperature range. The hydrocarbon data show that the α_e are large at room temperature, being 1.1×10^{-6}, 1.2×10^{-6}, and 2.4×10^{-6} cm^3 s^{-1} for CH_5^+, $C_2H_5^+$, and $C_6H_7^+$, respectively, and exhibit significant dependencies on temperature consistent with theoretical models based on the direct and indirect mechanisms. The change between these two dependencies occurs at a temperature of ∼300 K. The dissociative recombination of these ions is significant to molecular synthesis in interstellar clouds and the ionosphere of Titan, which is to be probed by the NASA Huygens-Cassini spacecraft that reaches the Saturnian system in July 2004. The relevance of the present data to these media is briefly discussed.

Introduction

Dissociative electron−ion recombination is the dominant mechanism for decay of ionization in many plasmas.[1,2] Electron−ion recombination, recently reviewed by Adams and coworkers[3], shows that the majority of recombination rate coefficients (α_e) have been obtained at room temperature, and only in cases such as Ne_2^+, Ar_2^+, Kr_2^+, Xe_2^+, NO^+, N_2^+, $H_3O^+(H_2O)_x$, (where $x = 1-5$), $NH_4^+(NH_4)_x$, (where $x = 1-4$), $N_2^+ \cdot N_2$, $CO^+ \cdot CO$, $CO^+ \cdot (CO)_2$, $O_2^+ \cdot O_2$, H_3^+, O_2^+, N_2H^+, and HCO^+ has temperature-dependent information been obtained.[3−6] Generally though, this information is not sufficiently detailed for temperature dependencies to be deduced. This is unfortunate, since mechanistic information can be obtained from such data. Also temperature-dependent data for hydrocarbon ions are critical in modeling the chemistry of the interstellar medium[7] and the Titan ionosphere.[8] To alleviate these problems, temperature dependencies have been determined for hydrocarbon ions of varying complexity (CH_5^+, $C_2H_5^+$, and $C_6H_7^+$ protonated benzene). Early theories of Bates[9] and Bardsley[1,10] predicted temperature dependencies of $T_e^{-0.5}$ and $T^{-1.5}$ for the direct and indirect processes, respectively, where T_e is the electron temperature.

The direct and indirect processes both involve a doubly excited dissociating state of the neutral molecule. The direct mechanism, which can be represented for CH_5^+ by

$$e^- + CH_5^+ \rightleftharpoons CH_5^{**} \rightarrow \text{neutral products} \qquad (1)$$

proceeds with the electron being captured directly onto a repulsive, dissociative potential curve of the excited neutralized ion. This is a dielectronic capture, where the recombining electron excites an electron in the ion, and this is resonantly captured with the incident electron to form the doubly excited neutral repulsive state CH_5^{**}. This state can initially autoionize back to the reactants, but as the products start to separate along the repulsive curve, the energy is converted from potential energy into kinetic energy of separation, soon making autoionization energetically unfavorable and dissociation inevitable.[3]

The indirect process proceeds through an additional intermediate step corresponding to a radiationless electron capture into a Rydberg level CH_5^*, e.g.,

$$e^- + CH_5^+ \rightleftharpoons CH_5^* \rightleftharpoons CH_5^{**} \rightarrow \text{neutral products} \qquad (2)$$

where the binding distance between the electron and the CH_5^+ core is large. This state undergoes a second radiationless transition to the same repulsive state as in the direct process, CH_5^{**}, which then dissociates. Recently, theoretical effort has been concentrated on calculating potential curves for individual systems and determining the probabilities of transitions at curve crossings.[11,12] Note, though, that recent theories have included quantum tunneling,[13] so that the absence of a curve crossing does not necessarily preclude rapid recombination.[14] Detailed approaches can, at present, only be applied to systems with up to about four atoms and have not been used for the hydrocarbon systems under consideration here. Fortunately, and surprisingly in the present study, the temperature dependencies are consistent with the simpler direct and indirect theoretical approaches as discussed below. The simple mechanistic behavior of these recombinations has enabled generalizations to be made about the recombination coefficients and their temperature dependence to facilitate the modeling of interstellar molecular clouds and the Titan ionosphere.

Experiment

The measurements were made using a variable-temperature flowing afterglow apparatus equipped with an axially movable Langmuir probe (VT-FALP). The apparatus has an available

* To whom correspondence should be addressed. Telephone: (706)-542-3722. Fax: (706)-542-9454. E-mail: adams@chem.uga.edu.

10.1021/jp040215l CCC: $27.50
Published on Web 07/16/2004

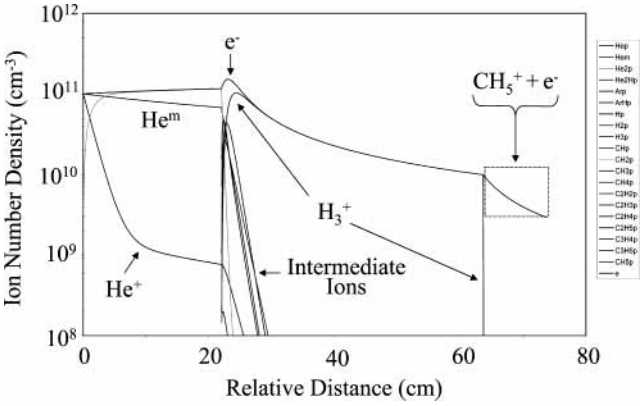

Figure 1. Mathematica model of the ion chemistry occurring as a function of distance along the flow tube for generation of CH_5^+ ions. The inset box is where CH_5^+ recombination occurs and is where the measurements of electron density (Figure 2) are performed to determine α_e. The α_e value for H_3^+ recombination used in the model was 1.10×10^{-7} cm^3 s^{-1}; larger or smaller literature values of this controversial recombination only slightly affect the ionization density at point where the hydrocarbons are added to the flow.[34]

TABLE 1: Literature Rate Coefficients (in cm^3 s^{-1} and cm^6 s^{-1} for the Termolecular Reactions) Used in the Kinetic Model[17,18,34]

reactant ion	reactant neutral	product ion	reaction rate coefficient (300 K)
He^+	He + He	He_2^+	1.00×10^{-31}
He^+	Ar	Ar^+	1.00×10^{-13}
He^+	H_2	(17%) H_2^+ (83%) H^+	1.00×10^{-13}
He^m	Ar	Ar^+	7.04×10^{-11}
He_2^+	Ar	Ar^+	2.00×10^{-10}
He_2^+	H_2	He_2H^+	5.30×10^{-10}
Ar^+	H_2	ArH^+	8.90×10^{-10}
H_2^+	Ar	ArH^+	2.10×10^{-9}
H^+	H_2 + He	H_3^+	1.50×10^{-29}
H_2^+	H_2	H_3^+	2.00×10^{-9}
ArH^+	H_2	H_3^+	6.30×10^{-10}
He_2H^+	H_2	H_3^+	3.00×10^{-10}
H_3^+	CH_4	CH_5^+	2.30×10^{-9}
CH_5^+	$CH_4 + CH_4$	$CH_5^+ \cdot CH_4$	8.00×10^{-30}
H_3^+	C_2H_6	$C_2H_5^+$	2.40×10^{-9}
$C_2H_5^+$	C_2H_6	products	4.00×10^{-11}
H_3^+	C_6H_6	$C_6H_7^+$	3.00×10^{-9}
$C_6H_7^+$	C_6H_6	N/A[a]	N/A
H_3^+	e^-	N/A	1.10×10^{-7}

[a] N/A indicates not available.

temperature range of 80−600 K. This type of technique has been described in detail previously[15,16] and will therefore be only briefly described here. A microwave discharge was used to create ionization in a flowing helium carrier gas (at about 2 Torr) generating helium cations He^+, helium metastables He^m, and electrons. At this pressure, helium cations are converting to He_2^+ by ternary association.[17] Hydrogen was then injected into the afterglow of the discharge, and this reacted with He_2^+ and He^m to give H_3^+ as the dominant ion. The ion chemistry was verified with a downstream quadrupole mass spectrometer, and supported by detailed models (Figure 1) of the ion chemistry involving numerically solving the differential rate equations of these systems. The reaction rate coefficients used in the models are given in Table 1.[17,18] Argon was often added upstream to destroy the helium metastables, and through this process several intermediate ions are created. These ions correspond to the concentrations, in Figure 1, that become negligible as H_3^+ becomes dominant. The H_3^+ concentration then tracks the electron density until the point at which, in this case, CH_4 is added.

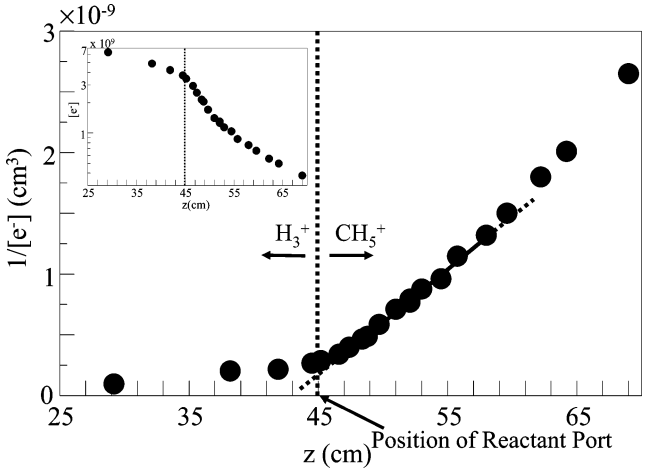

Figure 2. Plot of $1/[e^-]$ vs distance, z, for the electron−ion recombination of CH_5^+ used to determine the recombination rate coefficient (α_e) in conjunction with eq 7. The reactant port, where the hydrocarbons enter the flow, is identified by the vertical dotted line, and the arrows point to the regions where either H_3^+ or CH_5^+ ions dominate. The inset $[e^-]$ vs distance shows the $\ln[e^-]$ variation along the length of the flow tube.

The hydrocarbon gases and vapors (CH_4, C_2H_6, and C_6H_6) were introduced individually into the flow through one of several injector ports positioned along the flow tube. The model (Figure 1) confirms that the hydrocarbons were added where H_3^+ was the dominant cation. H_3^+ is known to react rapidly with these neutral hydrocarbons by the proton transfers (dissociative in the case of the C_2H_6 reaction),[19]

$$H_3^+ + CH_4 \rightarrow CH_5^+ + H_2 \quad (3)$$

$$H_3^+ + C_2H_6 \rightarrow C_2H_5^+ + 2H_2 \quad (4)$$

$$H_3^+ + C_6H_6 \rightarrow C_6H_7^+ + H_2 \quad (5)$$

and then the product ions begin to recombine with electrons. Secondary reactions in these systems such as three-body association of the type

$$CH_5^+ + CH_4 + CH_4 \rightarrow CH_5^+ \cdot CH_4 + CH_4 \quad (6)$$

were also included in the modeling to confirm that only the recombining ion of interest was present. The electron density, $[e^-]$, was determined as a function of position along the flow tube, using a Langmuir probe (25 μm diameter, 4 mm long) operating in the orbital limited region.[20] Pressures were used that were high enough to inhibit diffusion, thus making recombination the only significant loss process. This allowed a simple analysis[16] with a dependence of $[e^-]$ on axial position (z) of the form

$$\frac{1}{[e^-]_{t,z}} - \frac{1}{[e^-]_0} = \alpha_e \frac{z}{v} \quad (7)$$

where v is the ion velocity and z is the axial position along the flow tube. This method of analysis was used for all cases presented in this study; an example of data for the recombination of CH_5^+ is presented in Figure 2. In the inset, the slow decay of electron density upstream of the hydrocarbon addition point can be attributed to a combination of ambipolar diffusion of electrons and H_3^+ to the walls of the flow tube and slow recombination of H_3^+ ions. The upward curvature of the $1/[e^-]$ data, after the recombination regime, occurs because at lower electron densities diffusion dominates recombination as the

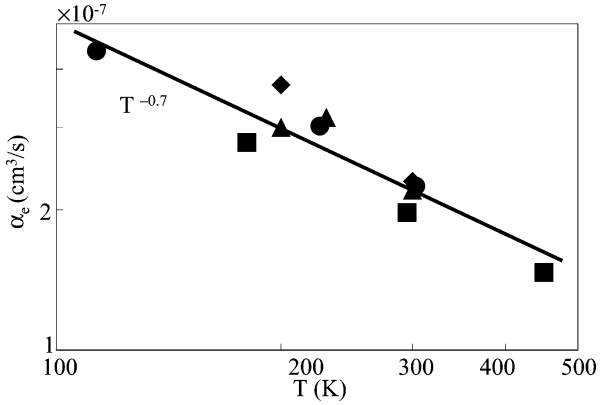

Figure 3. ln−ln plot of α_e vs temperature for O_2^+ dissociative recombination with electrons. The circles indicate the present data, and the squares,[5] diamonds,[35] and triangles[23] represent previous data in the literature.

TABLE 2: Measured Recombination Coefficients of O_2^+ Ions with Electrons; *x* Is the Power Law Index for the Temperature Dependence, T^{-x}

α_e ($cm^3\ s^{-1}$) at 300 K	*x*	temp (K)	method	ref
$2.24 \pm 0.3 \times 10^{-7}$	0.7	100−500	FALP	present data
$1.95 \pm 0.2 \times 10^{-7}$	0.7	300−1200	μWA-MS[a]	5
1.95×10^{-7}	0.7	200−600	FALP	35
1.95×10^{-7}	0.66	200−5000	trap[b]	23

[a] Microwave Afterglow-Mass Spectrometer. [b] Ion trap.

process for [e^-] decay. By performing a linear least-squares fit on this plot in the region where recombination is dominant, the recombination rate coefficient (α_e) can be evaluated using eq 7.[3] All recombination coefficients are accurate at 300 K to within ±15%, and ±20% at all other temperatures.

Results and Discussion

The temperature dependence of the O_2^+ recombination (shown in Figure 3) was determined to validate the technique since this recombination has been studied previously in detail.[5,21−23,35] Measurements were made at a series of temperatures ranging from 80 to 500 K to establish the temperature dependence. Table 2 lists the present and previous α_e at 300 K and the power of the temperature dependence. Figure 3 also shows these data for the recombination of O_2^+, which established an overall temperature dependence. The agreement gives confidence in our technique since the magnitudes of the difference between the various data are within experimental error.

Temperature dependencies for the CH_5^+, $C_2H_5^+$, and $C_6H_7^+$ recombinations are plotted in Figures 4−6, respectively. Data for the recombination of hydrocarbon ions was obtained over the same temperature range as for O_2^+ except for $C_6H_7^+$ for which studies were not possible at temperatures below 300 K due to condensation of benzene. The hydrocarbon ions are in their vibrational ground states from collisional relaxation due to the symmetrical proton transfer.

$$CH_5^+* + CH_4 \rightarrow CH_4* + CH_5^+ \qquad (8)$$

The CH_5^+ and $C_2H_5^+$ plots (Figures 4 and 5) show previous α_e data at 300 K that are greater than the ±15% error mentioned earlier. However, for CH_5^+, α_e data falls neatly within the range of the previous data. To our knowledge, detailed modeling of these systems was not conducted in the previous studies, and the hydrocarbon concentrations used may have been such that

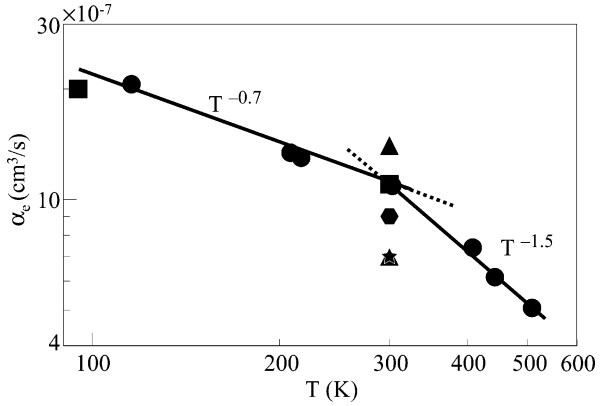

Figure 4. ln−ln plot of α_e vs temperature for CH_5^+ recombination with the circles indicating the present data, and the squares,[6] triangles,[36] hexagons,[37] and stars[38] representing previous data.

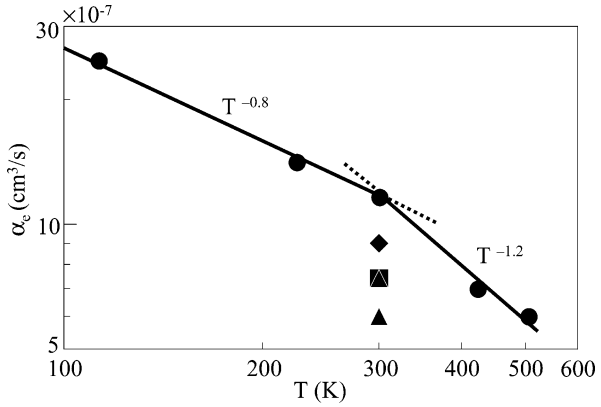

Figure 5. ln−ln plot of α_e vs temperature for $C_2H_5^+$ recombination with the circles indicating the present experimental data, and the square,[6] triangles,[36] diamond[37] representing previous 300 K data.

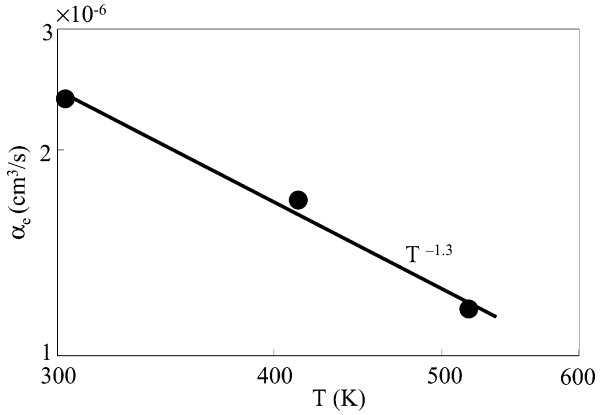

Figure 6. ln−ln plot of α_e vs temperature for $C_6H_7^+$.

precursor ion or cluster ion recombination were occurring to some degree. This was not the case with the present data. All data (see Figures 4−6) show similar behavior with higher slopes on ln−ln plots at high temperatures and lower slopes at low temperature. The exponents for these power law dependencies and the α_e at 300 K are listed in Table 3. The values for the low temperature region are somewhat above that generally suggested for direct process and that for the high-temperature region are approaching that for the indirect process. This is not unexpected since there can be a contribution of the indirect mechanism at low temperatures and the direct mechanism at high temperatures, enhancing and depressing the exponent, respectively. Note in Table 3 that for CH_5^+ and $C_2H_5^+$ the change-over between the two mechanisms occurs around 300

TABLE 3: Present Measured Recombination Coefficients and Temperature Dependencies in the Low and High Temperature Regimes for CH_5^+, $C_2H_5^+$, and $C_6H_7^+$ Ions; Power Law Index (x) in the T^{-x} Temperature Dependence Is Also Indicated

		power law index		change over
ion	α_e ($cm^3\,s^{-1}$) at 300 K	low temp	high temp	temp (K)
CH_5^+	$1.1 \pm 0.2 \times 10^{-6}$	0.7	1.5	300
$C_2H_5^+$	$1.2 \pm 0.2 \times 10^{-6}$	0.8	1.2	300
$C_6H_7^+$	$2.4 \pm 0.4 \times 10^{-6}$	N/A[a]	1.3	≤300

[a] N/A indicates not available.

K and that for $C_6H_7^+$ is below or at 300 K. Interestingly, no such change occurs for O_2^+ and a dependency around $T^{-0.7}$ has always been obtained over the whole temperature range. In examining the combined data, a pattern emerges with power law dependencies of $T^{-0.7\ \text{to}\ -0.8}$ at low temperatures and $T^{-1.2\ \text{to}\ -1.5}$ at high temperatures. There is some consistency of these rate coefficient data with other hydrocarbon data in the literature on the recombination of $C_2H_3^+$ and $C_3H_7^+$ determined using storage rings.[24,25] Here cross-sections are actually measured and converted into rate coefficients by integrating over a thermal Maxwell Boltzmann speed distribution. For the $C_2H_3^+$ recombination, the dependence is similar to the present study with $T^{-0.84}$ at low temperatures (50−1000 K) and $T^{-1.38}$ at high temperatures (1000−13000 K), with a break at ∼1000 K, somewhat higher than the present study.[25] For the $C_3H_7^+$ recombination,[24] there is a single dependence from 10 to 1000 K of $T^{-0.68}$. The bulk of the present and previous data, though, gives a dependence slightly steeper than the direct mechanism at low temperatures and slightly less than the indirect mechanism at high temperature. This discussion assumes that the direct and indirect mechanisms are independent; however, they are actually coupled with both being accessed in a single recombination. Mixing of these two mechanisms would thus be expected to result in different power law dependencies in the regions where they separately dominate, as is observed. In an early paper,[26] Bardsley was not able to determine the relative contributions of the two processes; however, this is automatically done in multichannel quantum defect theory MQDT.[22] To our knowledge, MQDT theory has not been applied to studies involving hydrocarbon ions. In light of the present data, theoretical determinations of the temperature dependencies and of the temperature at which the power law dependence changes would be valuable. The overall magnitude of α_e for these hydrocarbon ions is relatively similar. There is only a slight increase in the magnitude of α_e between CH_5^+ and $C_2H_5^+$, but as the hydrocarbon complexity increases to $C_6H_7^+$ the recombination rate increases by about a factor of 2.

The ionosphere of Titan has been modeled in the higher altitude region most recently by Fox and Yelle[8] and at lower altitudes by Molina-Cuberos et al.[27] To model the individual ion densities and the overall ionization/electron density, knowledge of the magnitude of the rate coefficients and their temperature dependencies is required. Fox and Yelle assumed, when there was little experimental data, that the recombination coefficients varied as $(3-3.5) \times 10^{-7}(300/T_e)^{0.5}$ $cm^3\ s^{-1}$, and Molina-Cuberos et al. similarly assumed for hydrocarbon ions $(5-8) \times 10^{-7}(300/T_e)^{0.5} cm^3\ s^{-1}$ (the slightly larger value assumed is realistic in view of the greater ionic complexity at lower altitudes). It is now necessary for the model calculations to be repeated to take into account the larger values obtained in the present study, which will make a significant difference to the ionization balance at the lower temperatures of the Titan ionosphere. Our generic temperature dependences for hydrocarbon ions would be $(300/T)^{0.7}$ below 300 K and $(300/T)^{1.4}$ above 300 K, with 300 K values of $(1-2) \times 10^{-6}$ $cm^3\ s^{-1}$. Thus, at the lowest temperatures in the Titan atmosphere of 100 K, the models of Fox and Yelle and Molina-Cuberos would suggest $(5.2-6.1) \times 10^{-7}$ $cm^3\ s^{-1}$ and $(8.7-13.9) \times 10^{-7}$ $cm^3\ s^{-1}$, respectively, with the present data giving $(23-68) \times 10^{-7}$ $cm^3\ s^{-1}$.

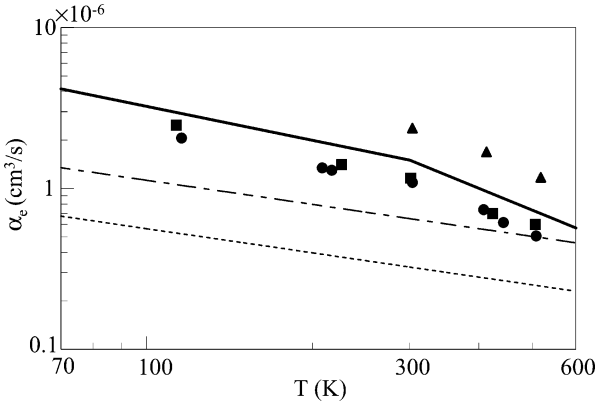

Figure 7. ln−ln plot of α_e vs temperature for CH_5^+ (circles), $C_2H_5^+$ (squares), and $C_6H_7^+$ (triangles) recombination. The Fox and Yelle model temperature dependence (dotted line), the Molina-Cuberos et al. model temperature dependence (dot−dash line), and our generic temperature dependence (solid line) are indicated.

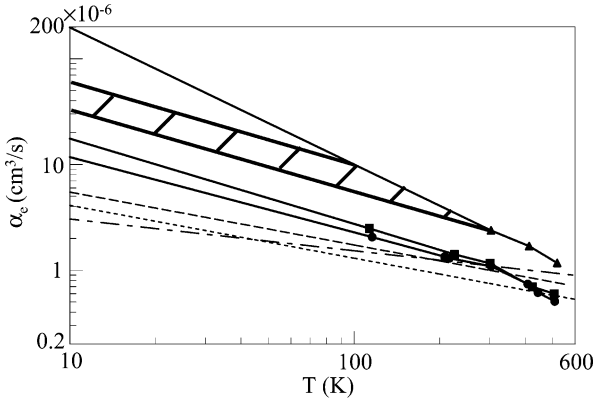

Figure 8. ln−ln plot of α_e vs temperature for CH_5^+ (circles), $C_2H_5^+$ (squares), and $C_6H_7^+$ (triangles) recombination extrapolated to 10 K, assuming a change over in mechanism between 100 and 300 K for $C_6H_7^+$. The UMIST[31] temperature dependence for CH_5^+ (dot−dash line), $C_2H_5^+$ (dotted line), $C_6H_7^+$ (dashed line) extrapolated from previous, very limited data are included.

All of these dependencies are shown in Figure 7 where a substantial difference is evident. If the power law dependencies refer to the direct and indirect mechanisms, then the changeover might be expected to be related to the temperature at which there is a significant population of vibrationally excited Rydberg states. Note that for O_2^+ all the data are in the low-temperature regime not inconsistent with the larger vibrational spacing relative to the hydrocarbon ions. However, this does not occur for all small non-hydrocarbon species. For example N_2H^+ shows little temperature dependence over the temperature range 80−500 K.[28] However, this may be a special case since there is evidence for quantum tunneling in this recombination,[28,29] These data indicate important trends for α_e variations with temperature and contain insights into the mechanisms involved.

The recombinations are also significant to interstellar chemistry with the detection of now over 20 hydrocarbon species.[30] The formation of these molecules occurs either within the molecular clouds themselves or in the expanding envelopes of

old stars.[7] Here, at the lower temperatures of ~10 K, α_e values based on extrapolation of the present data are 1.2×10^{-5} and 1.8×10^{-5} cm^3 s^{-1} for CH_5^+ and $C_2H_5^+$, respectively, compared with extrapolation of UMIST data,[31] (usually a single or perhaps two data points), which would yield 3.1×10^{-6} and 4.1×10^{-6} cm^3 s^{-1} for CH_5^+ and $C_2H_5^+$, respectively. Shown in Figure 8 are the extrapolated temperature dependencies. Figure 8 also shows the extrapolated dependence of recombination for $C_6H_7^+$. An assumed change in temperature dependence between 100 and 300 K was used since it was not possible to observe this for $C_6H_7^+$; this yields a α_e of $(3.0-6.0) \times 10^{-5}$ cm^3 s^{-1} at 10 K. Assuming no change in the mechanism for $C_6H_7^+$ yields a α_e of 2.0×10^{-4} cm^3 s^{-1}, while the UMIST dependence would yield a α_e of 5.5×10^{-6} cm^3 s^{-1} at 10 K. The interstellar models need to be recalculated with the new data to make them more realistic.

Conclusions

The data presented here imply a generic temperature-dependent behavior for electron−ion recombination of hydrocarbon ions, and this is now being extended to other hydrocarbon ions. This is important since such recombinations are relevant to the synthesis of neutral hydrocarbons in the interstellar clouds and the atmospheric chemistry of Titan.[8] In the upper atmosphere, the ions suggested by the Fox and Yelle model are $C_2H_5^+$, CH_5^+, and $HCNH^+$ in order of decreasing abundance, and thus the recombination of the two most abundant ions has been studied here.

Determining recombination rate coefficients as a function of temperature will continue with emphasis being placed on more complex organic molecules which exist in interstellar space[30,32] and extraterrestrial atmospheres,[33] such as that of Titan. The data presented above indicate that these recombination rate coefficients follow a combination of mechanisms. In the absence of detailed theory for these systems, the rate coefficients must be measured directly to ensure accurate values for inclusion in the models.

Acknowledgment. Funding under NASA Grant No. NAG5-8951 is gratefully acknowledged.

References and Notes

(1) Bardsley, J. N.; Biondi, M. A. *Adv. At. Mol. Phys.* **1970**, *6*, 1.
(2) Smith, D.; Adams, N. G. *Pure Appl. Chem.* **1984**, *56*, 175.
(3) Adams, N. G.; Babcock, L. M.; McLain, J. L. Electron-Ion Recombination. In *Encyclopedia of Mass Spectrometry: Theory and Ion Chemistry*; Armentrout, P., Ed.; Elsevier: Amsterdam, 2003; Vol. 1, p 542.
(4) Adams, N. G.; Smith, D.; Alge, E. *J. Chem. Phys.* **1984**, *81*, 1778.
(5) Johnsen, R. *Int. J. Mass Spectrom. Ion Processes* **1987**, *81*, 67.
(6) Adams, N. G.; Smith, D. Laboratory Studies of Dissociative Recombination and Mutual Neutralization and their Relevance to Interstellar Chemistry. In *Rate Coefficients in Astrochemistry*; Millar, T. J., Williams, D. A., Eds.; Kluwer: Dordrecht, 1988; p 173.
(7) Herbst, E. *Adv. Gas Phase Ion Chem.* **1998**, *3*, 1.
(8) Fox, J. L.; Yelle, R. V. *Geophys. Res. Lett.* **1997**, *24*, 2179.
(9) Bates, D. R. *Phys. Rev.* **1950**, *78*, 492.
(10) Bardsley, J. N. *J. Phys. B* **1968**, *1*, 365.
(11) Talbi, D. *Dissociative Recombination of C-$C_3H_3^+$*; Kluwer: New York, 2003.
(12) Guberman, S. L. *The Dissociative Recombination of N_2^+*; Kluwer: New York, 2003.
(13) Bates, D. R. Dissociative Recombination: Crossing and Tunneling Modes. In *Advances in Atomic, Molecular and Optical Physics*; Bederson, B., Walther, H., Eds.; Academic Press: San Diego, 1994; Vol. 34, p 427.
(14) Bell, R. P. *The Tunnel Effect in Chemistry*; Chapman and Hall: London 1980.
(15) Smith, D.; Adams, N. G. Studies of Plasma Reaction Processes using a Flowing Afterglow/Langmuir Probe Apparatus. In *Swarms of Ions and Electrons in Gases*; W., L., Mark, T. D., Howorka, F., Eds.; Springer-Verlag: Vienna, 1984; p 284.
(16) Adams, N. G.; Smith, A. D. Flowing Afterglow and SIFT. In *Techniques for the Study of Ion-Molecule Reactions*; Farrar, J. M., Saunders, J. W. H., Eds.; John Wiley & Sons: NY, 1988; Vol. 20; p 165.
(17) Ikezoe, Y.; Matsuoka, S.; Takebe, M.; Viggiano, A. A. *Gas-Phase Ion-Molecule Reaction Rate Constants through 1986*; Ion Reaction Research Group of the Mass Spectroscopy Society of Japan: Tokyo, 1987.
(18) Anicich, V. *An Index of the Literature for Bimolecular Gas-Phase Cation-Molecule Reaction Kinetics*; Jet Propulsion Laboratory: Pasadena, 2003.
(19) Milligan, D. B.; Wilson, P. F.; Freeman, C. G.; Meot-Ner, M.; McEwan, M. J. *J. Phys. Chem. A* **2002**, *106*, 9745.
(20) Swift, J. D.; Schwar, M. J. R. *Electrical Probes for Plasma Diagnostics*; Iliffe: London, 1970.
(21) Smith, D.; Goodall, C. V. *Planet. Space Sci.* **1968**, *16*, 1177.
(22) Giusti, A. *J. Phys. B* **1980**, *13*, 3867.
(23) Walls, F. L.; Dunn, G. H. *J. Geophys. Res.* **1974**, *79*, 1911.
(24) Ehlerding, A.; Arnold, S. T.; Viggiano, A. A.; Kalhori, S.; Semaniak, J.; Derkatch, A. M.; Rosen, S.; af Ugglas, M.; Larsson, M. *J Phys. Chem. A* **2003**, *107*, 2179.
(25) Kalhori, S.; Viggiano, A. A.; Arnold, S. T.; Rosen, S.; Semaniak, J.; Derkatch, A. M.; af Ugglas, M.; Larsson, M. *Astron. Astrophys.* **2002**, *391*, 1159.
(26) Bardsley, J. N. *J. Phys. B* **1968**, *1*, 349.
(27) Molina-Cuberos, G. J.; Lopez-Moreno, J. J.; Rodrigo, R. *Geophys. Res.* **1999**, *104*, 21997.
(28) Poterya, V.; McLain, J. L.; Adams, N. G.; Babcock, L. M. *J Phys. Chem.* **2004**. Manuscript in preparation.
(29) Butler, J. M.; Babcock, L. M.; Adams, N. G. *Mol. Phys.* **1997**, *91*, 81.
(30) McCarthy, M. C.; Thaddeus, P. *Chem. Soc. Rev.* **2001**, *30*, 177.
(31) Le Teuff, Y. H.; Millar, T. J.; Markwick, A. J. *Astron. Astrophys., Suppl. Ser.* **2000**, *146*, 157.
(32) Adams, N. G.; Babcock, L. M.; Ray, N. S. Ionic Processes in Low-Temperature Interstellar Molecular Plasmas. In *Atomic Processes in Plasmas*; Schultz, D. R., Meyer, F. W., Ownby, F., Eds.; AIP: Melville, NY, 2002; p 182.
(33) Fox, J. L.; Yelle, R. V. *Geophys. Res. Lett.* **1997**, *24*, 2179.
(34) Plasil, R.; Glosik, J.; Poterya, V.; Kudrna, P.; Rusz, J.; Tichy, M.; Pysanenko, A. *Int J. Mass Spectrom.* **2002**, *218*, 105.
(35) Alge, E.; Adams, N. G.; Smith, D. *J. Phys. B* **1983**, *16*, 1433.
(36) Mitchell, J. B. A.; Rebrion-Rowe, C. *Int. Rev. Phys. Chem.* **1997**, *16*, 201.
(37) Gougousi, T.; Golde, M. F.; Johnsen, R. *Chem. Phys. Lett.* **1997**, *265*, 399.
(38) Lehfaoui, L.; Rebrion-Rowe, C.; Laube, S.; Mitchell, B. A.; Rowe, B. R. *J. Chem. Phys.* **1997**, *106*, 5406.